D. Nikitin, I. Omelchenko, A. Zakharova, M. Avetyan, A. L. Fradkov, E. Schöll

# Complex partial synchronization patterns in networks of delay-coupled neurons



Nikitin, D., Omelchenko, I., Zakharova, A., Avetyan, M., Fradkov, A. L., & Schöll, E. (2019). Complex partial synchronization patterns in networks of delay-coupled neurons. Philosophical Transactions of the Royal Society A: Mathematical, Physical and Engineering Sciences, 377(2153), 20180128. https://doi. org/10.1098/rsta.2018.0128

PHILOSOPHICAL TRANSACTIONS A

rsta.royalsocietypublishing.org

Research

Article submitted to journal

**Subject Areas:**
applied mathematics, mathematical modelling

**Keywords:**
neural networks, chimera states, multiplex networks, delay coupling

**Author for correspondence:**
Eckehard Schöll
e-mail: schoell@physik.tu-berlin.de

# Complex partial synchronization patterns in networks of delay-coupled neurons

D. Nikitin[1], I. Omelchenko[2], A. Zakharova[2], M. Avetyan[1], A.L. Fradkov[1,3] and E. Schöll[2]

[1]Saint Petersburg State University, Saint Petersburg, Russia
[2]Institut für Theoretische Physik, Technische Universität Berlin, 10623 Berlin, Germany
[3]Institute for Problems of Mechanical Engineering, Saint Petersburg, Russia

We study the spatiotemporal dynamics of a multiplex network of delay-coupled FitzHugh-Nagumo oscillators with nonlocal and fractal connectivities. Apart from chimera states, a new regime of coexistence of slow and fast oscillations is found. An analytical explanation for the emergence of such coexisting partial synchronization patterns is given. Furthermore we propose a control scheme for the number of fast and slow neurons in each layer.

## 1. Introduction

The control of nonlinear dynamical systems and networks has evolved into a wide interdisciplinary area of research over the past decades [1–3]. Synchronization phenomena in networks [4–7] are of great importance in many areas ranging from physics and chemistry to biology, neuroscience, physiology, ecology, socio-economic systems, computer science, and engineering. Chaos synchronization of lasers, for instance, may lead to new secure communication schemes [8–10]. The synchronization of neurons is believed to play a crucial role in the brain under normal conditions, for instance in the context of cognition and learning [11], and under pathological conditions such as Parkinson's disease [12]. Neuronal synchronization can also be induced by white or colored external noise [13]. Fireflies are known to synchronize their flashing [14]. Synchronization of power grids is essential for their operation [15].

Time delay effects are a key issue in realistic networks. For example, the finite propagation time of light between coupled semiconductor lasers [16–21] significantly influences the dynamics. Similar effects occur in neuronal networks [22,23]. Time delay has two complementary, counterintuitive and almost contradicting facets. On the one hand, delay is able to induce instabilities, bifurcations of periodic and quasiperiodic orbits, multistability and chaotic motion. On the other hand, delay can suppress instabilities, stabilize unstable stationary or periodic states and may control deterministic chaos. Both facets open up efficient methods of designing and controlling nonlinear dynamics by time-delayed feedback [2,24].

To determine the stability of a synchronized state in a network of identical units, a powerful method has been developed [25], i.e., the master stability function. This approach has been extended to networks with coupling delays [26–32], where the master stability function depends non-trivially on delay times. There exist different forms of synchronization, i.e., complete or isochronous (zero-lag) synchronization, generalized synchronization, cluster or group synchronization [31,33–36], and many other forms. Some progress has been made in generalizing this work, for instance, towards adaptive control [37], inhomogeneous local dynamics [38] and heterogeneous delay times [39], distributed [40,41], state-dependent, or time-varying delays [42]. In general, the stability of synchronization in delay-coupled networks of oscillators depends in a complicated way on the local dynamics of the nodes and the coupling topology. However, for large coupling delays synchronizability relates in a simple way to the spectral properties of the network topology, characterized by the eigenvalue spectrum of the coupling matrix. The master stability function used to determine the stability of synchronous solutions has a universal structure in the limit of large delay: it is rotationally symmetric and increases monotonically with the radius in the complex plane. This allows for a universal classification of networks with respect to synchronization properties [29]. For smaller coupling delays the synchronization properties depend in a more subtle way upon the local dynamics, and the details of the network topology. Various cluster synchronization states, where certain clusters inside the network show isochronous synchronization, can be realized by tuning the coupling parameters such as the coupling phase, coupling strength, and delay time [27,31]. To find appropriate values of these control parameters, the speed-gradient method from control theory can be applied to achieve a desired state of generalized synchrony (*adaptive synchronization*) [37,43,44]. Transitions between synchronization and desynchronization can be induced by introducing inhibitory links into an excitable regular network with a probability $p$ in a small-world like fashion, and changing the balance between excitatory and inhibitory links. This has been demonstrated for different generic local dynamics of the nodes, and various coupling topologies like rings, small-world, and random networks. In particular, oscillatory local dynamics (the Stuart-Landau oscillator, i.e., a generic expansion near a Hopf bifurcation), type-I excitable dynamics (near a saddle-node bifurcation on an invariant cycle, or *saddle-node infinite period* (SNIPER) bifurcation), and type-II excitable dynamics (the FitzHugh-Nagumo model) have been considered [45,46].

Recent interest has focussed on more complex partial synchronization patterns, which cannot be described by simple approaches like the master stability method. These synchronization patterns may include self-sustained coherent or incoherent oscillations, and other parts where the oscillations are quenched. Two types of oscillation quenching mechanisms, i.e., amplitude death and oscillation death, have been intensely studied both theoretically and experimentally [47–50]. Amplitude death is associated with the stabilization of an already existing trivial steady state while oscillation death is characterized by a newly born inhomogeneous steady state. The extensions of the studies of these global phenomena towards partial amplitude and oscillation death [48,51,52] are first steps towards a better understanding of the emergence of local mesoscale structures on networks and their influence on the global dynamics [53–57].

A very prominent example of partial synchronization patterns are chimera states, i.e., symmetry-breaking states of partially coherent and partially incoherent behavior, for recent reviews see [58,59]. Chimera states are intriguing spatio-temporal patterns made up of

spatially separated domains of synchronized (spatially coherent) and desynchronized (spatially incoherent) behavior, although they arise in networks of completely identical units. Kuramoto et al. discovered the chimeras in a network of phase oscillators with a simple symmetric non-local coupling scheme [60]. Within these "classical" chimera states, coherent domains of periodic in-phase oscillations coexist with incoherent domains, characterized by a chaotic behavior in time and space. In Greek mythology, the chimera is a fabulous creature with a lion's, a goat's, and a snake's head. As the counterintuitive dynamical state is as well composed of incongruous parts, it was named after the beast [61]. In real-world systems chimera states might play a role, e.g., in the unihemispheric sleep of birds and dolphins [62,63], see also recent computer simulations with empirical connectivities of human brains [64], in epileptic seizures [65–69], in power grids [15], or in social systems [70]. Time-delayed feedback or coupling has been shown to be a versatile method for controlling chimera states in networks of Stuart-Landau oscillators [71], Van der Pol oscillators [72], or FitzHugh-Nagumo oscillators [73,74].

Recently, much research has been devoted to multilayer networks, which provide a description of systems interconnected through different types of links. The interplay of intra-layer interaction with inter-layer coupling opens up a plethora of phenomena in different fields, e.g. [75–78]. In neural systems, multilayer networks represent, for instance, neurons in different areas of the brain or neurons connected either by a chemical link or by an electrical synapsis [79,80]. A special case of multilayer networks are multiplex topologies, where each layer contains the same set of nodes, and only pairwise connections between corresponding nodes from neighbouring layers exist [81–86].

In this paper we study the dynamics of two-layer neural networks using the FitzHugh-Nagumo model [87,88] in the oscillatory regime with inter-layer coupling delay. The FitzHugh-Nagumo model is paradigmatic for neuronal systems which show excitability of type II, i.e., are close to a Hopf bifurcation [89]. In [90,91] the dynamics of two coupled FitzHugh-Nagumo systems with time-delayed feedback was considered in different regimes. In [92] it was shown that chimera states can emerge in a single ring of FitzHugh-Nagumo oscillators with nonlocal coupling. Here we focus on two coupled rings with different coupling topologies, namely fractal connectivities, which have been associated in the literature with neuronal systems [93], and compact nonlocal coupling, which has been extensively studied as a simple paradigmatic topology for chimera states. Our motivation is to investigate the paradigmatic interaction of these two typical neuronal architectures, fractal and compact, respectively, in a two-layer configuration. This might help to better understand the mechanisms of real-world brain dynamics; as an example we refer to [69], where we have compared the dynamics for an empirical neural connectivity matrix prepared from real human diffusion-weighted magnetic resonance imaging (MRI) data with an artificial fractal connectivity matrix with the aim to explain epileptic seizures.

In section 2 the model is presented. Section 3 discusses different synchronization patterns which emerge in the network. In particular, the slow-fast coexistence state is introduced for the case where the inter-layer coupling is stronger than the intra-layer coupling. In this state some neurons oscillate essentially with the frequency of a single FitzHugh-Nagumo system, while others have almost doubled their frequency. Section 4 is devoted to the mapping of the various regimes in parameter space. In Section 5 the nature of the slow-fast coexistence state is investigated, and analytical results are derived.

An important aspect of this work is to study possibilities for control of two-layer networks (Section 6). Previous work on control of two-layer networks was mostly devoted to control of the inter-layer synchronization [94]. However, in our case the coupling between the layers is stronger than the coupling of neurons within one layer. Therefore inter-layer synchronization is always observed and the control goal is different. Our analysis indicates that the number of neurons with doubled frequency, which depends on the initial conditions, may be controlled. It is shown in Section 6(a) that the intra-layer coupling strengths are appropriate parameters for such control. Therefore the rest of Section 6 is devoted to the design of control algorithms to achieve

the maximum or minimum number of fast and slow neurons in each layer. To this end the speed-gradient (SG) method [95,96] is applied and SG algorithms in the difference form are proposed. Some numerical evidence of the feasibility of such an approach to control of two-layer networks is presented.

## 2. Model

The FitzHugh-Nagumo (FHN) oscillator is a paradigmatic model for neural systems [87,88]. The uncoupled dynamics of each node in the network is given by

$$\begin{pmatrix} \varepsilon \dot{u} \\ \dot{v} \end{pmatrix} = F(u,v), \qquad F(u,v) = \begin{pmatrix} u - \frac{u^3}{3} - v \\ u + a \end{pmatrix}, \tag{2.1}$$

where $u$ and $v$ are activator and inhibitor variables, respectively, $\varepsilon > 0$ is a small parameter characterizing the time scale separation between the fast activator and the slow inhibitor, and the threshold parameter $a \in \mathbb{R}$ defines the excitable ($|a| > 1$) or oscillatory ($|a| < 1$) regime. We use $\varepsilon = 0.05$ and $a = 0.5$ throughout this work as in [92].

To obtain chimera states, in [92] nonlocal coupling of each node on a ring to its $P$ neighbors to the left and to the right, respectively, was used. If $N$ is the total number of oscillators, $r = P/N$ is the dimensionless coupling radius.

We consider a two-layer network with different connectivity structure in the two layers (see scheme in Fig. 1). Layer one (top) is chosen to be nonlocal with coupling radius $r = P/N = 0.35$ and coupling strength $\sigma_1 = 0.1$. For layer two (bottom) a fractal connectivity is used as described in [74]. It is constructed in an iterative hierarchical way by a Cantor algorithm using a base pattern (an initiation string) of zeros and ones of length $b = 3$, where each element represents either a link ('1') or a gap ('0'). In our case this pattern is (101). In each iterative step, each link is replaced by the initial base pattern, while each gap is replaced by $b$ gaps. Thus, each iteration increases the size of the final bit pattern, such that after $n$ iterations the total length is $N = b^n$. In front of the resulting string an additional zero is placed, corresponding to absent self-coupling. Using the resulting string as the first row of the adjacency matrix $G$, and constructing a circulant adjacency matrix $G$ by applying this string to each element of the ring, a ring network of $N = b^n + 1$ nodes (in our case after 5 iteration steps $N = 3^5 + 1 = 244$) with (quasi)fractal or hierarchical connectivity is generated [97,98]. We use the same coupling strength in the second layer $\sigma_2 = 0.1$. In both layers the intra-layer coupling of the activator and inhibitor variables is through a $2 \times 2$ rotational matrix

$$R(\phi) = \begin{pmatrix} \cos\phi & \sin\phi \\ -\sin\phi & \cos\phi \end{pmatrix} \tag{2.2}$$

depending on the coupling phase $\phi \in [-\pi, \pi)$. It was shown [92] that chimeras can be found for nonlocal coupling when $\phi$ is close to $\pi/2$ (we use $\phi = \pi/2 - 0.1$), corresponding to dominant activator-inhibitor cross-coupling, which is a common mechanism in neuroscience, see, e.g., the recent review on different functional interactions [99]. Also, chimeras depend on $\sigma$ and $r$; in particular for $\sigma = 0.1$ chimeras arise for $r$ between 0.25 and 0.43.

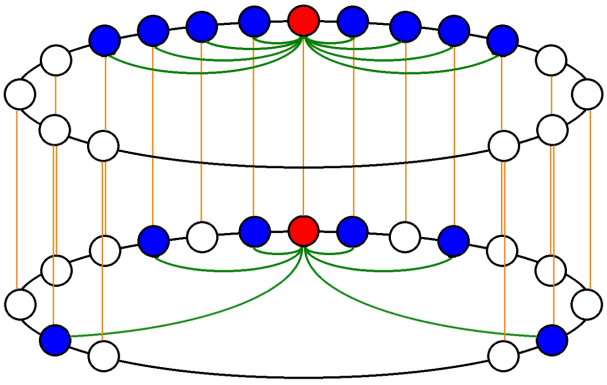

**Figure 1.** Scheme of the two-layer network with different layer topologies (top: nonlocal, bottom: fractal connectivities)

The two layers are only coupled vertically through corresponding nodes, thus creating a multiplex network. The inter-layer coupling is via the $u$ variables, with coupling strength $\sigma_{12}$ and coupling delay $\tau$. We assume that the intra-layer coupling delay can be neglected compared to the internal time scale of the FHN system, while the inter-layer coupling delay is larger and cannot be neglected. Thus, the dynamics of the network is given by:

$$\begin{aligned}
\begin{pmatrix} \varepsilon \dot{u}_{i,1} \\ \dot{v}_{i,1} \end{pmatrix} &= F(u_{i,1}, v_{i,1}) + \frac{\sigma_1}{2rN} \sum_{|j-i| \leqslant rN} R(\phi) \begin{pmatrix} u_{j,1} - u_{i,1} \\ v_{j,1} - v_{i,1} \end{pmatrix} + \sigma_{12} \begin{pmatrix} u_{i,2}(t-\tau) - u_{i,1} \\ 0 \end{pmatrix}, \\
\begin{pmatrix} \varepsilon \dot{u}_{i,2} \\ \dot{v}_{i,2} \end{pmatrix} &= F(u_{i,2}, v_{i,2}) + \frac{\sigma_2}{|G_i|} \sum_{G_{ij}=1} R(\phi) \begin{pmatrix} u_{j,2} - u_{i,2} \\ v_{j,2} - v_{i,2} \end{pmatrix} + \sigma_{12} \begin{pmatrix} u_{i,1}(t-\tau) - u_{i,2} \\ 0 \end{pmatrix}.
\end{aligned} \tag{2.3}$$

Here in $u_{i,m}, v_{i,m}$ the subscripts denote the intra-layer node index $i$, and the layer number $m$, respectively, and $|G_i|$ denotes the row sum of the matrix $G_{ij}$. As initial conditions throughout this work we use a chimera state obtained from a previous simulation with random initial phases on a circle of radius 2 in the $(u, v)$-plane in layer 1, and constant $(u, v)$ = (1.3321, 0.5745) for all neurons in layer 2.

## 3. Synchronization Patterns in the Network

We investigate our system by varying the inter-layer coupling strength $\sigma_{12}$ and the coupling delay $\tau$, and observe the emerging spatio-temporal patterns. First of all, for sufficiently large inter-layer coupling $\sigma_{12}$ (say, $\sigma_{12} > 0.02$) the patterns in both layers become identical. In section 4 numerical results supporting this proposition will be given.

We find two stable patterns that can arise in such a network, depending upon the parameters. First of all, a *chimera state* characterized by the coexistence of synchronized and desynchronized domains and by an arc-shaped mean frequency profile. Second, we obtain a pattern in which some neurons oscillate with a frequency twice as large as the others. We call this pattern *slow-fast coexistence*.

To characterize the spatial coherence and incoherence we use the real-valued local order parameter

$$Z_{k,n} = \frac{1}{2\delta} \left| \sum_{|j-k| \leqslant \delta} e^{i\Theta_{k,n}} \right|, \qquad n \in \{1, 2\}, \tag{3.1}$$

where $\Theta_{k,n} = \arctan(v_{k,n}/u_{k,n})$ is the geometric phase, and $\delta = 15$ is the size of the local averaging window.

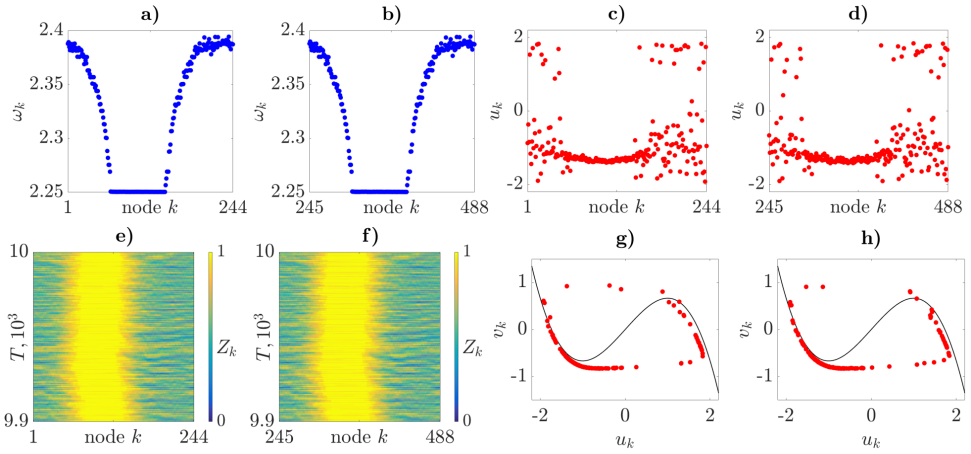


**Figure 2.** Chimera pattern. **a-b)** Arc-shaped mean frequency profiles. **c-d)** Snapshots of $u_k$ for $t = 10^4$. **e-f)** Space-time plot, where the local order parameter $Z_k$ (3.1) is color coded. **g-h)** Snapshots in the $(u_k, v_k)$ phase plane for $t = 10^4$ (black curve is the $u$ nullcline of the single FHN system). In each double panel the left part corresponds to layer one, and the right part corresponds to layer two. Parameters: $N = 244$, $\varepsilon = 0.05$, $a = 0.5$, $r = 0.35$, $\phi = \pi/2 - 0.1$, $\sigma_1 = \sigma_2 = \sigma_{12} = 0.1$, $\tau = 0.5$.

In Fig. 2 a chimera pattern is shown. In this case $\sigma_{12} = 0.1$ and $\tau = 0.5$. It can be clearly seen that the mean frequency profile $\omega$ has the common arc-shaped form, with the synchronized domains (flat) in both layers at the same location in the center.

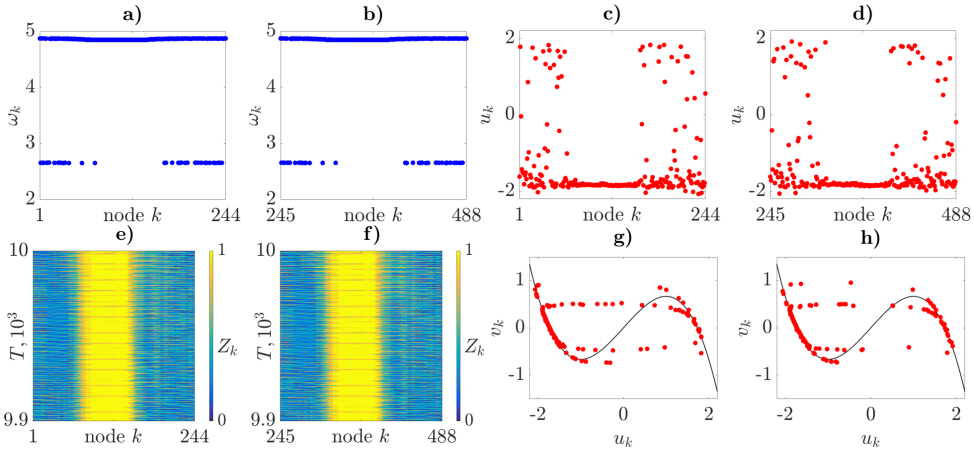


**Figure 3.** Slow-fast coexistence pattern. Same plots as in Fig. 2 for different inter-layer coupling $\sigma_{12}$ and delay $\tau$. Parameters: $N = 244$, $\varepsilon = 0.05$, $a = 0.5$, $r = 0.35$, $\phi = \pi/2 - 0.1$, $\sigma_1 = \sigma_2 = 0.1$, $\sigma_{12} = 0.4$, $\tau = 1.2$.

In Fig. 3 a coexistence pattern of slow and fast neuronal oscillations is shown. Here $\sigma_{12} = 0.4$ and $\tau = 1.2$. In Fig. 3a-b one can see that some neurons have a mean frequency $\omega_k$ close to 5

(we call them *fast* neurons), while others have a mean frequency close to 2.5 (we call them *slow* neurons). The snapshots Fig. 3c-d and the space-time plots of the local order parameter Fig. 3e-f clearly show two coexisting domains of synchronized dynamics (center) and incoherent behavior, but the characteristic arc-shaped mean frequency profile of chimeras is absent; instead there are only two discrete frequencies whose spatial sequence in the incoherent domain is random. Also, in Fig. 3g-h the snapshot in the phase plane shows two distinct limit cycles, one with larger sections on the slow manifolds (active phase and recovery phase), corresponding to the full limit cycle of the single FHN system, and one with shortened sections on the slow manifolds (approximately double frequency). Analogous shortening of the duty cycle (and hence reduced period, i.e., increased frequency) has been observed in an opto-electronic delay oscillator with similar null isocline [100] and in a single FHN oscillator with delayed feedback [101].

## 4. Map of Regimes

Here we map out the types of pattern in the $(\sigma_{12}, \tau)$ plane, see Fig. 4a for $\sigma_{12} \in \{0.0125...0.5\}$ and $\tau \in \{0.075...3\}$. From the map one can see that slow-fast coexistence (red) can arise only with $\tau$ close to half of the intrinsic period $T_0 = 2.67$ of a single FHN oscillator. Also sufficiently high inter-layer coupling strength $\sigma_{12} > 0.1$ is needed. Note that chimera states (white) always exist, indicating bistability.

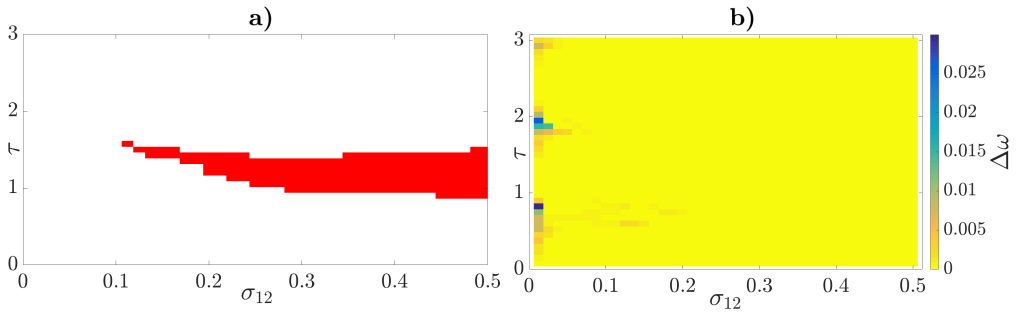


**Figure 4. a)** Map of regimes for the slow-fast coexistence state (red). The chimera state (white) always exists, indicating bistability. **b)** Mean frequency deviation $\Delta\omega$ between the two layers in the $(\sigma_{12}, \tau)$ plane. Parameters: $N = 244$, $\varepsilon = 0.05$, $a = 0.5$, $r = 0.35$, $\phi = \pi/2 - 0.1$, $\sigma_1 = \sigma_2 = 0.1$.

It is interesting that the *slow-fast* characteristic of the neurons $(u_{i,n}, v_{i,n})$ always applies simultaneously to the pair of neurons $(u_{i,1}, v_{i,1})$ and $(u_{i,2}, v_{i,2})$. This is because the mean frequency profiles of both layers are similar: if $\omega_{i,1}$ is high, $\omega_{i,2}$ will also be high. To show this, we use a measure of the frequency deviation:

$$\Delta\omega = \max_{i \in \{1...N\}} |\omega_{i,1} - \omega_{i,2}|. \tag{4.1}$$

In Fig. 4b the dependence of $\Delta\omega$ on $\sigma_{12}$ and $\tau$ is shown. For all considered values of $\sigma_{12}$ and $\tau$ $\Delta\omega < 0.03$. Moreover, for the region of slow-fast coexistence (Fig. 4a) $\Delta\omega < 0.005$. This means that neurons with the same intra-layer subscript cannot have different *slow-fast* characteristics. $\Delta\omega$ only increases when $\sigma_{12} \to 0$.

# 5. Analytical Results

In this section we will give an explanation for the existence of two frequencies for certain $\sigma_{12}$ and $\tau$ values. Also we will show that this characteristic always applies to the pair of neurons in the two layers.

## (a) A single Neuron with Delayed Feedback

We will start by considering one FitzHugh-Nagumo neuron with delayed self-coupling:

$$\begin{cases} \varepsilon \dot{u} = u - \dfrac{u^3}{3} - v + \sigma\left(u(t-\tau) - u\right), \\ \dot{v} = u + a. \end{cases} \tag{5.1}$$

Again, we fix $\varepsilon = 0.05$, $a = 0.5$. Also we choose $\sigma = 0.4$ as in Fig. 3. If we start with $\tau = 0$ and then increase $\tau$, at some point the neuron $(u(t), v(t))$ starts to follow the virtual delayed neuron $(u(t-\tau), v(t-\tau))$ on the limit cycle, whereas the limit cycle itself becomes smaller. This effect is shown in Fig. 5a. Note that in [101] a similar model is studied, but it is operated in the excitable regime ($a > 1$), and the analysis is performed for small delay $\tau = O(\varepsilon)$.

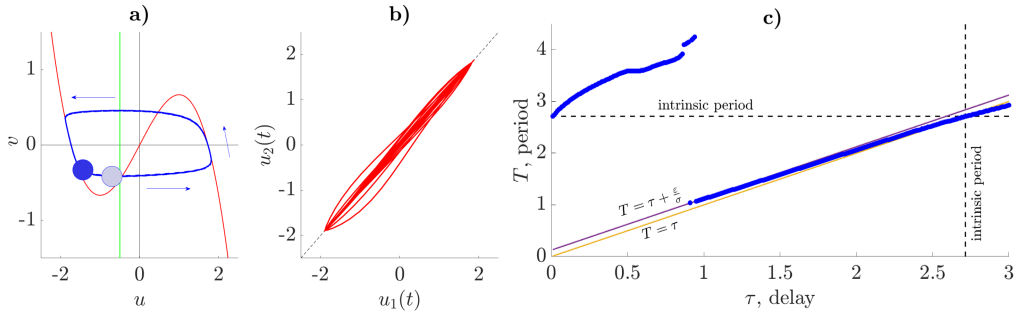


**Figure 5. a)** Limit cycle for a single FitzHugh-Nagumo oscillator with delayed feedback for $\tau = 1.2$ in the $(u, v)$ plane. Limit cycle period $T = 1.31$. The dark blue dot denotes the real neuron $(u(t), v(t))$, and the light blue dot is a delayed neuron $(u(t-\tau), v(t-\tau))$. **b)** Phase plane $(u_1, u_2)$ for a pair of in-phase neurons. **c)** Dependence of period $T$ on delay $\tau$ for the FHN oscillator with delayed feedback (blue dots). Solid lines: theoretical bounds (5.3). Parameters: $\varepsilon = 0.05$, $a = 0.5$, $\sigma = 0.4$. The history function (initial condition) is chosen as constant for $t \in [-\tau, 0]$.

The fact that the delayed neuron is slightly ahead of the real neuron means that the difference $h = T - \tau$ between period $T$ and delay $\tau$ is small. When the system is on a stable limit cycle, $u(t) = u(t+T)$. This means that $u(t-\tau) = u(t+T-\tau) = u(t+h)$. Considering small $h$, we can approximate $u(t+h) \approx u(t) + h\dot{u}(t)$. Then the dynamic equations become

$$\begin{cases} (\varepsilon - \sigma h)\dot{u} = u - \dfrac{u^3}{3} - v, \\ \dot{v} = u + a. \end{cases} \tag{5.2}$$

This is equivalent to an undelayed FHN system with rescaled $\bar{\varepsilon} = \varepsilon - \sigma h$. It is obvious that $\bar{\varepsilon} > 0$ needs to hold. Thus we obtain the inequality $h = T - \tau < \varepsilon/\sigma$. This argument assumes that the delayed neuron is slightly ahead of the real neuron. It results in the following inequality giving

upper and lower bounds for the period of the limit cycle:

$$\tau < T < \tau + \frac{\varepsilon}{\sigma}. \tag{5.3}$$

Inequality (5.3) predicts the numerically obtained dependence of $T$ on $\tau$ which is shown in Fig. 5c. Starting from $\tau = 0.97$ up to the intrinsic period $\tau = T_0 = 2.67$, a very good approximation of the period $T$ is obtained.

## (b) Two Delay-Coupled Neurons

Now let us consider a system of two FHN neurons coupled with delay [90,102]:

$$\begin{cases} \varepsilon \dot{u}_1 = u_1 - \dfrac{u_1^3}{3} - v_1 + \sigma\left(u_2(t-\tau) - u_1\right), \\ \dot{v}_1 = u_1 + a, \\ \varepsilon \dot{u}_2 = u_2 - \dfrac{u_2^3}{3} - v_2 + \sigma\left(u_1(t-\tau) - u_2\right), \\ \dot{v}_2 = u_2 + a. \end{cases} \tag{5.4}$$

The parameters $\varepsilon = 0.05$, $a = 0.5$, $\sigma = 0.4$ are the same as in the previous case.

If $u_1 \approx u_2$ and $v_1 \approx v_2$ as initial conditions, the two neurons will synchronize, and their limit cycle will be the same as for one neuron with delayed feedback. Also, if we depict the trajectory $(u_1(t), u_2(t))$ in the phase plane, it will converge to the line $u_1 \equiv u_2$, see Fig. 5b.

For a system of two neurons also anti-phase dynamics is possible [90], when the two neurons are initially at antipodal positions, and the delay time is approximately half the period, i.e., each neuron is slightly behind the delayed version of the other neuron. This is shown in Fig. 6a.

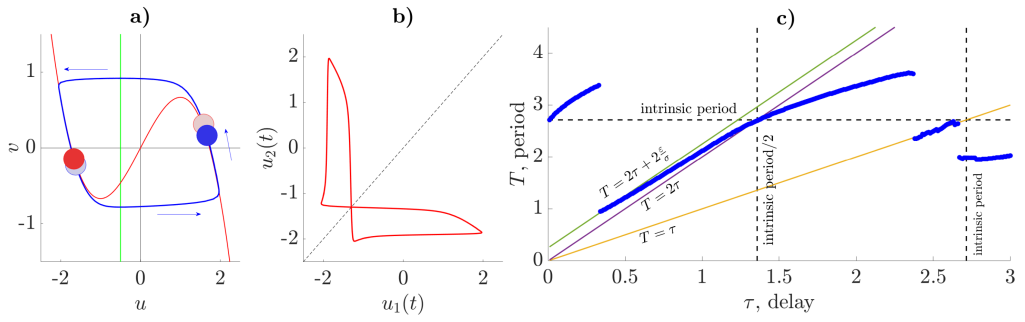


**Figure 6. a)** Limit cycle for two delay-coupled FitzHugh-Nagumo neurons for $\tau = 1.2$ in the $(u, v)$ plane. Limit cycle period $T = 2.55$. The dark blue dot denotes the real neuron $(u_1(t), v_1(t))$, the dark red dot is the real neuron $(u_2(t), v_2(t))$, the light blue dot is the delayed neuron $(u_1(t-\tau), v_1(t-\tau))$, and the light red dot is the delayed neuron $(u_2(t-\tau), v_2(t-\tau))$. **b)** Phase plane $(u_1, u_2)$ for a pair of anti-phase neurons. **c).** Dependence of $T$ on $\tau$ for two delay-coupled FHN oscillators (blue dots). Solid lines: theoretical bounds (5.5). Parameters: $\varepsilon = 0.05$, $a = 0.5$, $\sigma = 0.4$. Initial conditions: The first neuron is placed at $(u_1, v_1)$=(1.7, 0) (i.e, in the middle of the right slow manifold in phase space), and the second neuron is placed at the antipodal position (-1.7, 0). The history function is chosen as constant for $t \in [-\tau, 0]$.

The anti-phase dynamics shows up as a butterfly-like trajectory $(u_1(t), u_2(t))$ in the phase plane, see Fig. 6b. Again, on the limit cycle $u_1(t) = u_1(t+T) = u_2(t+T/2)$. We can choose $h = T/2 - \tau$, then $u_1(t-\tau) = u_2(t+T/2-\tau) = u_2(t+h)$. The first order approximation gives $u_1(t-\tau) \approx u_2(t) + h\dot{u}_2(t)$. Thus, system (5.4) separates into two independent systems of the type

of (5.2), which again gives the inequality $h < \varepsilon/\sigma$. Recalling the definition of $h$, we obtain

$$2\tau < T < 2\tau + 2\frac{\varepsilon}{\sigma}. \tag{5.5}$$

The numerical dependence of $T$ on $\tau$ is shown in Fig. 6c. Inequality (5.5) holds from $\tau = 0.34$ up to half of the intrinsic period $\tau = T_0/2 = 1.34$.

## (c) Application to the Two-Layer Network

Our results from subsections (a) and (b) show that there exist some values of $\tau$ for which two delay-coupled FHN neurons can exhibit two different types of dynamics with different frequencies, depending on the realization of the initial conditions. Each pair of neurons (one in layer 1 and the other in layer 2) has approximately equal probability of being in-phase or anti-phase, and each realization may give a different dynamics, i.e., a different sequence of slow (anti-phase) and fast (in-phase) oscillators within each layer, thus the system is highly multistable. According to Fig. 5c and Fig. 6c, for $\sigma = 0.4$ and $\tau \in [0.97, 1.34]$ the period $T$ can be estimated either by (5.3) (in-phase) or by (5.5) (anti-phase).

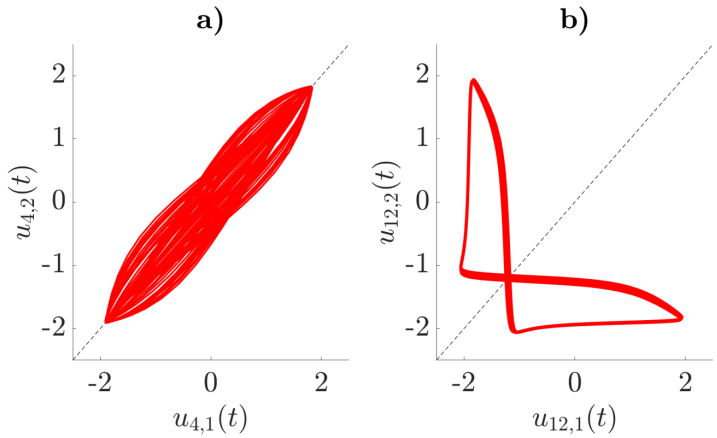


**Figure 7.** Phase planes $(u_1, u_2)$ for two pairs of neurons in the two-layer network. **a)** Pair of neurons $(u_{4,1}(t), v_{4,1}(t))$ and $(u_{4,2}(t), v_{4,2}(t))$, which belongs to the fast class (in-phase, mean frequency $\omega_4 = 4.87$). **b)** Pair of neurons $(u_{12,1}(t), v_{12,1}(t))$ and $(u_{12,2}(t), v_{12,2}(t))$, which belongs to the slow class (anti-phase, mean frequency $\omega_{12} = 2.68$).

Those neurons who follow (5.3) have almost double frequency as those who follow (5.5). Hence the fast class in the two-layer network corresponds to in-phase dynamics, while the slow class is associated with anti-phase dynamics. To verify this, we show exemplary phase planes $(u_1, u_2)$ for the full network. In Fig. 7 panel a) depicts the trajectory $(u_{4,1}(t), u_{4,2}(t))$. This trajectory tends to the line $u_1 \equiv u_2$, as in Fig. 5b. Neuron $(u_{4,1}(t), v_{4,1}(t))$ has mean frequency $\omega_4 = 4.87$, thus belonging to the fast class. At the same time, Fig. 7b shows the trajectory $(u_{12,1}(t), u_{12,2}(t))$, which is clearly of the "butterfly" shape, as in Fig. 6b. Neuron $(u_{12,1}(t), v_{12,1}(t))$ has mean frequency $\omega_{12} = 2.68$ and belongs to the slow class. This is in good agreement with previous numerical results for two delay-coupled neurons [90].

Also, one can see that the limit cycles in Fig. 5a and Fig. 6a perfectly match with the phase space snapshots in Fig. 3g-h, where two limit cycles coexist.

Throughout this paper we choose the coupling radius equal to $r = 0.35$, since the regime where chimeras occur is centered around values close to $r = 1/3$ (see [92], Fig. 3). As long as we stay

in that regime, the results are robust. In general, the effect of slow-fast coexistence should not depend upon the intra-layer topology, since our analytical explanation of coexistence of slow-fast oscillations is independent of the intra-layer topologies and relies mainly on the delayed coupling of a pair of neurons, one from layer 1, the other from layer 2, thus this effect can be observed with many different network structures. For our choice of $N = 244$, the fractal connectivity network in layer two is much sparser than the compact nonlocally coupled network in layer one; actually, the intra-layer fractal connectivity string has only 32 non-zero connections for each neuron versus 162 connections for nonlocal coupling (for $r = 1/3$). For single-layer networks a careful analysis of the robustness of chimera states for FitzHugh-Nagumo oscillators with various coupling topologies, including different fractal connectivities, has established that the patterns are rather robust [97]. However, we have found slow-fast coexistence only in two-layer multiplex networks, due to the delayed coupling of pairs of neurons from the two layers. The successive elimination of links in the nonlocal coupling to make a stepwise transition from compact nonlocal to fractal connectivities has been systematically studied in a one-layer network in [98]. In order to investigate this transition for our two-layer model, we have performed simulations for the parameters of Fig. 3, but with $m = 1, 2, 3, 4$ iteration steps of the base pattern (101) in layer 2. For this purpose we have expanded the $m$-step bit pattern of size $3^m$ to a full final bit pattern of size $N = 3^5 + 1 = 244$ identical elements by replacing each element with $243/3^m$ copies of itself and again adding the additional zero in the first entry of the final pattern (corresponding to absent self-coupling), similar to [98]. The compact nonlocal coupling of layer 1 is kept fixed at $r = 1/3$. We find that the slow-fast patterns persist for all iteration steps $m = 1, 2, 3, 4, 5$, even for $m = 1$ which means identical compact nonlocal topologies in both layers. The results are displayed in Figs. 8 and 9 for $m = 1$ and $m = 3$, respectively. Note that both figures show two coherent domains, but the slow-fast frequency profiles are very similar to the case $m = 5$ shown in Fig. 3.

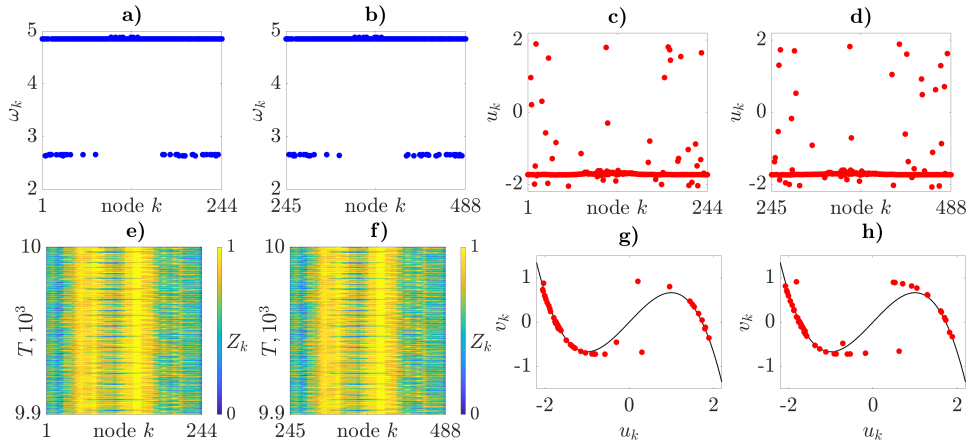


**Figure 8.** Slow-fast coexistence patterns for different topologies of layer 2. Same plots as in Fig. 3 for iteration step $m = 1$ of the base pattern (101) in layer 2, i.e., identical nonlocal topologies in both layers. Parameters: $N = 244$, $\varepsilon = 0.05$, $a = 0.5$, $r = 81/244 = 0.33$, $\phi = \pi/2 - 0.1$, $\sigma_1 = \sigma_2 = 0.1$, $\sigma_{12} = 0.4$, $\tau = 1.2$.

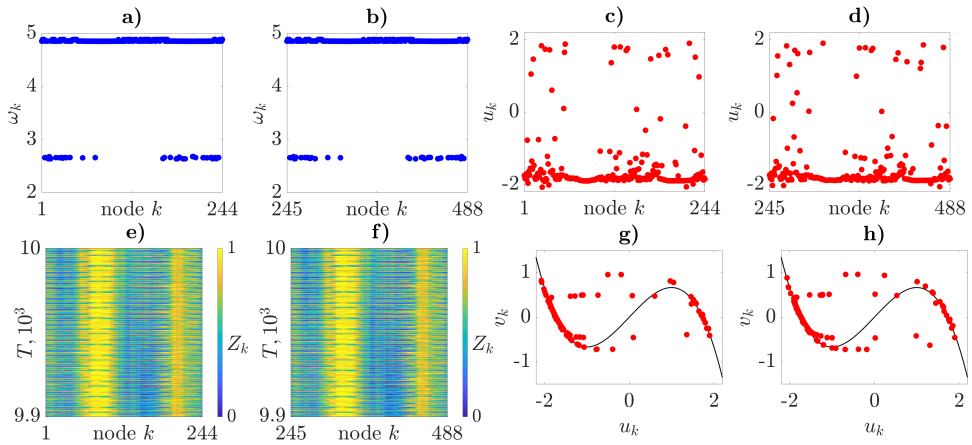


**Figure 9.** Slow-fast coexistence patterns for different topologies of layer 2. Same plots as in Fig. 3 for iteration step $m = 3$ of the base pattern (101) in layer 2. Parameters as in Fig. 8.

# 6. Control of the Two-Layer Network

## (a) Control of two delay-coupled oscillators

As shown in Section 5(c), the dynamics of the full network depends heavily on the properties of corresponding pairs of delay-coupled neurons (one in layer 1, the other in layer 2). These pairs can perform in-phase or anti-phase oscillations, depending on initial conditions, similar to two delay-coupled oscillators in Eq. (5.4). Our aim now is to select and stabilize either of these two behaviors, independently of initial conditions. For this purpose we use proportional control with control coefficient $K$ in the following form:

$$\begin{cases} \varepsilon \dot{u}_1 = u_1 - \dfrac{u_1^3}{3} - v_1 + \sigma\left(u_2(t-\tau) - u_1\right) + K(u_2 - u_1), \\ \dot{v}_1 = u_1 + a + K(v_2 - v_1), \\ \varepsilon \dot{u}_2 = u_2 - \dfrac{u_2^3}{3} - v_2 + \sigma\left(u_1(t-\tau) - u_2\right) + K(u_1 - u_2), \\ \dot{v}_2 = u_2 + a + K(v_1 - v_2). \end{cases} \tag{6.1}$$

$K = 0$ corresponds to the previous case (Section 5). For sufficiently large positive $K$ the anti-phase mode becomes unstable and in-phase dynamics arises even if the initial condition is chosen in anti-phase; numerical simulations show that it is sufficient to choose $K > 0.3$, see Fig. 10a. For negative $K$ the in-phase mode becomes unstable and anti-phase dynamics occurs even for symmetric initial conditions, see Fig. 10b. Therefore it is possible to control the type of synchronization (in-phase or anti-phase, corresponding to the fast and the slow periodic mode, respectively) of the system (5.4) by proportional control.

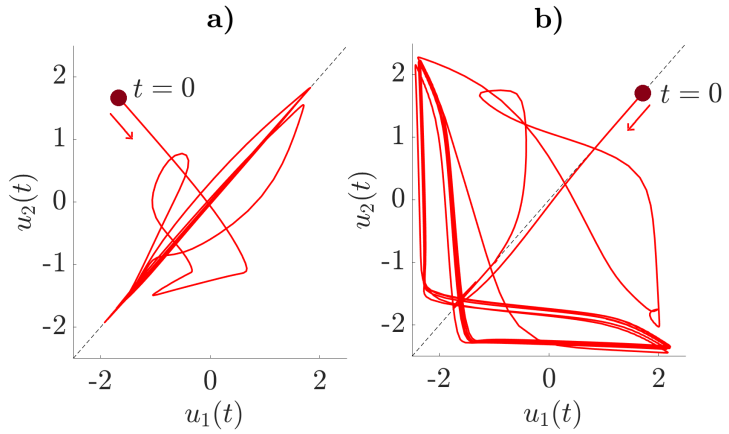


**Figure 10.** Proportional control of in-phase and anti-phase dynamics of two delay-coupled FHN oscillators: Phase plane $(u_1, u_2)$ for **a)** $K = 0.5$: Transition from anti-phase to in-phase; **b)** $K = -0.2$: Transition from in-phase to anti-phase. Other parameters: $\varepsilon = 0.05$, $a = 0.5$, $\sigma = 0.4$.

## (b) Control of Proportion between Slow and Fast Classes in the Network

The slow-fast coexistence state in the two-layer network arises when some neuron pairs oscillate in-phase, whereas others oscillate in anti-phase. The number of neurons in each class depends on the initial conditions. Since the proportion of the numbers in the slow and fast class determines the overall mean frequency of the network, it is important to find a way of controlling this ratio. For instance, in neuroscience different stages of sleep are associated with different frequencies of spiking neurons, and sleep regulation is controlled by the thalamocortical system [64].

To this purpose first we rewrite the network equations (2.3):

$$\begin{aligned}
\begin{pmatrix} \varepsilon \dot{u}_{i,1} \\ \dot{v}_{i,1} \end{pmatrix} &= \begin{pmatrix} u_{i,1} - \frac{u_{i,1}^3}{3} - v_{i,1} \\ u_{i,1} + a \end{pmatrix} + \sigma_1 \begin{pmatrix} \Delta_{i,1}^u \\ \Delta_{i,1}^v \end{pmatrix} + \sigma_{12} \begin{pmatrix} u_{i,2}(t-\tau) - u_{i,1} \\ 0 \end{pmatrix}, \\
\begin{pmatrix} \varepsilon \dot{u}_{i,2} \\ \dot{v}_{i,2} \end{pmatrix} &= \begin{pmatrix} u_{i,2} - \frac{u_{i,2}^3}{3} - v_{i,2} \\ u_{i,2} + a \end{pmatrix} + \sigma_2 \begin{pmatrix} \Delta_{i,2}^u \\ \Delta_{i,2}^v \end{pmatrix} + \sigma_{12} \begin{pmatrix} u_{i,1}(t-\tau) - u_{i,2} \\ 0 \end{pmatrix}.
\end{aligned} \tag{6.2}$$

Here $\Delta_{i,n}^u$ and $\Delta_{i,n}^v$ denote the cumulative intra-layer coupling effect of layer $n$ on neuron $i$:

$$\begin{pmatrix} \Delta_{i,1}^u \\ \Delta_{i,1}^v \end{pmatrix} = \frac{1}{2rN} \sum_{|j-i| \leqslant rN} R(\phi) \begin{pmatrix} u_{j,1} - u_{i,1} \\ v_{j,1} - v_{i,1} \end{pmatrix}, \qquad \begin{pmatrix} \Delta_{i,2}^u \\ \Delta_{i,2}^v \end{pmatrix} = \frac{1}{|G_i|} \sum_{G_{ij}=1} R(\phi) \begin{pmatrix} u_{j,2} - u_{i,2} \\ v_{j,2} - v_{i,2} \end{pmatrix} \tag{6.3}$$

To simplify the notation we define $x_i = u_{i,1} - u_{i,2}$ and $y_i = v_{i,1} - v_{i,2}$.

Parameters $\sigma_{12}$ and $\tau$ are crucial for the emergence of the slow-fast coexistence state (see map of regimes in Fig. 4a. In the following we fix them as $\sigma_{12} = 0.4$ and $\tau = 1.2$. In analogy with the instantaneous proportional control term with control coefficient $K$ in Subsection (a) we now use the cumulative instantaneous intra-layer coupling terms $\sigma_n \begin{pmatrix} \Delta_{i,n}^u \\ \Delta_{i,n}^v \end{pmatrix}$ in the role of control terms for the full network equations (6.2) with control parameters $\sigma_1$ and $\sigma_2$. We will develop a control algorithm using the speed-gradient method [95,96].

Given the general nonlinear dynamical system $\dot{z} = F(z, u)$, the speed-gradient method can be used to minimize a nonnegative function $Q(z)$, also known as goal function, along the trajectories of the system by properly choosing the control parameter $u$. In order to design a control algorithm,

the scalar function $\omega(z,u)=\dot{Q}$ is calculated along the trajectories:

$$\omega(z,u)=[\nabla_z Q(z)]^T F(z,u). \tag{6.4}$$

Then the gradient of $\omega(z,u)$ with respect to the control variable $u$ is evaluated as

$$\psi(z,u)=\nabla_u\left([\nabla_z Q(z)]^T F(z,u)\right). \tag{6.5}$$

Finally, the control function $u$ is obtained as

$$u=u_0-\gamma\psi(z,u) \tag{6.6}$$

with some control gain $\gamma>0$, and $u_0$ is the initial (reference) control value (often $u_0=0$ is assumed). Eq. (6.6) is called speed-gradient (SG) algorithm in finite form since it suggests to change $u$ proportionally to the gradient of the speed of changing $Q$. For the speed-gradient in its differential form see [96].

The idea of this algorithm is the following: The term $-\nabla_u\omega(z,u)$ points to the direction in which the value of $\dot{Q}$ decreases with the highest speed. Therefore, if one forces the control signal to "follow" this direction, the value of $\dot{Q}$ will decrease and finally be negative. When $\dot{Q}<0$, then $Q$ will decrease and, eventually, will tend to zero.

Let us now apply this control algorithm to the two-layer network. If we want to control the proportion between the numbers of fast and slow neurons, we can use the following strategy: we find two algorithms, one aimed at increasing the number of fast neurons and another one aimed at decreasing it. Then we apply these algorithms subsequently in order to get the desired value of proportion. The results from section 3 show that once we stop the control algorithms and fix the control parameters $\sigma_1$ and $\sigma_2$ to some constant values, the numbers of fast and slow neurons remain also constant.

To find the algorithm for increasing the number of fast neurons let us use the SG method with goal function

$$Q_f=\frac{1}{2}\sum_{i=1}^{N}\left(x_i^2+y_i^2\right). \tag{6.7}$$

This function should be zero if every neuron pair is in-phase, so minimizing it gives us the maximizum size of the fast class. Applying the SG method leads to the control algorithm

$$\begin{cases}\sigma_1=-\gamma\sum_{i=1}^{N}[x_i\Delta_{i,1}^u+y_i\Delta_{i,1}^v],\\ \sigma_2=\gamma\sum_{i=1}^{N}[x_i\Delta_{i,2}^u+y_i\Delta_{i,2}^v].\end{cases} \tag{6.8}$$

As shown above, the fast and the slow class correspond to in-phase and anti-phase oscillations, respectively, which can be used as an approximately instantaneous criterion for determining the size of the fast and the slow class. If a neuron pair is approximately in-phase, $|x_i|$ and $|y_i|$ should be small. Thus, we can use the number of nodes $K_{fast}$ with sufficiently small $|x_i|$ and $|y_i|$ as a measure of the size of the fast class:

$$K_{fast}=\#\{i:x_i^2+4y_i^2<2\}. \tag{6.9}$$

In order to have comparable magnitude of $x_i$ and $y_i$ we use $4y_i^2$. The evolution of $K_{fast}$ in the system with control (6.8) is shown in Fig. 11a. This plot shows significant oscillations of $K_{fast}$ on the time scale of one FHN period, because the measure of the size of the class is not strictly instantaneous. Asymptotically, all neurons are in the fast class.

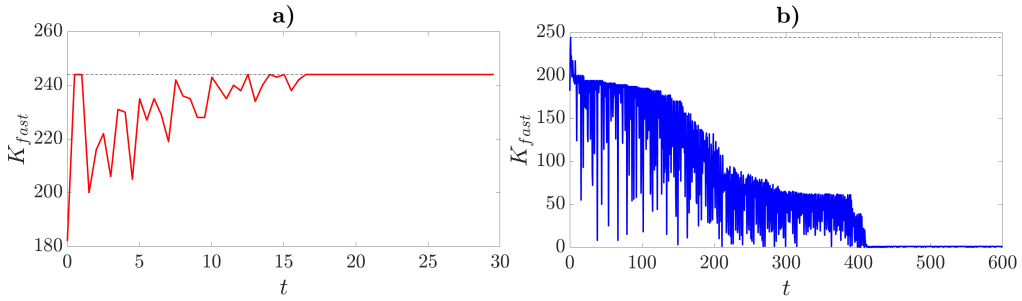


**Figure 11. a).** Control (6.8) for driving all neurons to the fast class. **b).** Control (6.11) for driving all neurons to the slow class. Parameters: $N = 244$, $\varepsilon = 0.05$, $a = 0.5$, $r = 0.35$, $\phi = \pi/2 - 0.1$, $\sigma_{12} = 0.4$, $\tau = 1.2$, $\gamma = 0.03$.

To obtain an algorithm for decreasing the number of fast neurons, we can use a different goal function:

$$Q_s = 2\sum_{i=1}^{N}\left(3 - \sqrt{|x_i|} - \sqrt{|y_i|}\right). \tag{6.10}$$

Here the constant 3 is used to guarantee nonnegativity, but it has no effect on the algorithm itself (any number $> 3$ can be chosen). Square roots are used since they give more weight to the neurons with small $|x_i|$ and $|y_i|$. Applying the speed-gradient method we obtain:

$$\begin{cases} \sigma_1 = \gamma\sum\limits_{i=1}^{N}\left[\dfrac{\operatorname{sign} x_i}{\sqrt{|x_i|}}\Delta^u_{i,1} + \dfrac{\operatorname{sign} y_i}{\sqrt{|y_i|}}\Delta^v_{i,1}\right], \\ \sigma_2 = -\gamma\sum\limits_{i=1}^{N}\left[\dfrac{\operatorname{sign} x_i}{\sqrt{|x_i|}}\Delta^u_{i,2} + \dfrac{\operatorname{sign} y_i}{\sqrt{|y_i|}}\Delta^v_{i,2}\right]. \end{cases} \tag{6.11}$$

Fig. 11b shows the measure for the size of the fast class $K_{fast}$ with this control algorithm. As in the previous case, the goal is asymptotically approached, i.e., no neurons are left in the fast class, but this requires slightly more time, because destabilizing the in-phase dynamics is more difficult.

Thus the proposed algorithms (6.8) and (6.11) allow to achieve the maximum and minimum values of $K_{fast}$, respectively, i.e., all nodes or no nodes, respectively, are in the fast class.

## 7. Conclusion

We have shown that in a two-layer network with delayed inter-layer coupling a new regime of coexistence of slow and fast oscillations can arise. We have found the regimes of existence in the plane of the inter-layer coupling strength and delay, and have proposed an analytical explanation. We have also designed a control algorithm to control the proportion between the numbers of slow and fast neurons in the network, and thereby control the overall mean frequency. Moreover, our study might open up further interesting directions of future research by analyzing the effects of other topologies in both layers.

Authors' Contributions. DN did the numerical simulations and the theoretical analysis. MA assisted in the simulations and analysis IO, AZ, AF and ES supervised the study. All authors designed the study and contributed to the preparation of the manuscript. All the authors have read and approved the final manuscript.

Competing Interests. The authors declare that they have no competing interests.

Funding. This work was supported by DFG in the framework of SFB 910 and by DAAD in the framework of G-RISC.

Acknowledgements. We are grateful to Jakub Sawicki for stimulating discussions.

## References


1. E. Schöll, S. H. L. Klapp, and P. Hövel: *Control of self-organizing nonlinear systems* (Springer, Berlin, 2016).
2. E. Schöll and H. G. Schuster (Editors): *Handbook of Chaos Control* (Wiley-VCH, Weinheim, 2008), second completely revised and enlarged edition.
3. A. L. Fradkov: *Horizons of cybernetical physics*, Phil. Trans. R. Soc. A **375**, 20160439 (2017).
4. A. Pikovsky, M. G. Rosenblum, and J. Kurths: *Synchronization: a universal concept in nonlinear sciences* (Cambridge University Press, Cambridge, 2001).
5. A. G. Balanov, N. B. Janson, D. E. Postnov, and O. V. Sosnovtseva: *Synchronization: From Simple to Complex* (Springer, Berlin, 2009).
6. V. I. Nekorkin: *Introduction to Nonlinear Oscillations* (Wiley, Weinheim, 2015).
7. S. Boccaletti, A. N. Pisarchik, C. I. del Genio, and A. Amann: *Synchronization: From Coupled Systems to Complex Networks* (Cambridge University Press, Cambridge, 2018).
8. K. M. Cuomo and A. V. Oppenheim: *Circuit implementation of synchronized chaos with applications to communications*, Phys. Rev. Lett. **71**, 65 (1993).
9. S. Boccaletti, J. Kurths, G. Osipov, D. L. Valladares, and C. S. Zhou: *The synchronization of chaotic systems*, Phys. Rep. **366**, 1 (2002).
10. I. Kanter, E. Kopelowitz, and W. Kinzel: *Public channel cryptography: chaos synchronization and Hilbert's tenth problem*, Phys. Rev. Lett. **101**, 84102 (2008).
11. W. Singer: *Neuronal Synchrony: A Versatile Code Review for the Definition of Relations?*, Neuron **24**, 49 (1999).
12. O. Popovych, M. N. Xenakis, and P. A. Tass: *The spacing principle for unlearning abnormal neuronal synchrony*, PLOS ONE **10**, 1 (2015).
13. S. Zambrano, I. P. Marino, J. M. Seoane, M. A. F. Sanjuán, S. Euzzor, A. Geltrude, R. Meucci, and F. T. Arecchi: *Synchronization of uncoupled excitable systems induced by white and coloured noise*, New J. Phys. **12**, 053040 (2010).
14. J. Buck and E. Buck: *Mechanism of rhythmic synchronous flashing of fireflies: Fireflies of southeast asia may use anticipatory time-measuring in synchronizing their flashing*, Science **159**, 1319 (1968).
15. A. E. Motter, S. A. Myers, M. Anghel, and T. Nishikawa: *Spontaneous synchrony in power-grid networks*, Nat. Phys. **9**, 191 (2013).
16. H. J. Wünsche, S. Bauer, J. Kreissl, O. V. Ushakov, N. Korneyev, F. Henneberger, E. Wille, H. Erzgräber, M. Peil, W. Elsäßer, and I. Fischer: *Synchronization of delay-coupled oscillators: A study of semiconductor lasers*, Phys. Rev. Lett. **94**, 163901 (2005).
17. T. W. Carr, I. B. Schwartz, M. Y. Kim, and R. Roy: *Delayed-mutual coupling dynamics of lasers: scaling laws and resonances*, SIAM J. Appl. Dyn. Syst. **5**, 699 (2006).
18. H. Erzgräber, B. Krauskopf, and D. Lenstra: *Compound laser modes of mutually delay-coupled lasers*, SIAM J. Appl. Dyn. Syst. **5**, 30 (2006).
19. I. Fischer, R. Vicente, J. M. Buldú, M. Peil, C. R. Mirasso, M. C. Torrent, and J. García-Ojalvo: *Zero-lag long-range synchronization via dynamical relaying*, Phys. Rev. Lett. **97**, 123902 (2006).
20. O. D'Huys, R. Vicente, T. Erneux, J. Danckaert, and I. Fischer: *Synchronization properties of network motifs: Influence of coupling delay and symmetry*, Chaos **18**, 037116 (2008).
21. M. C. Soriano, J. García-Ojalvo, C. R. Mirasso, and I. Fischer: *Complex photonics: Dynamics and applications of delay-coupled semiconductors lasers*, Rev. Mod. Phys. **85**, 421 (2013).
22. E. Rossoni, Y. Chen, M. Ding, and J. Feng: *Stability of synchronous oscillations in a system of Hodgkin-Huxley neurons with delayed diffusive and pulsed coupling*, Phys. Rev. E **71**, 061904 (2005).
23. C. Masoller, M. C. Torrent, and J. García-Ojalvo: *Interplay of subthreshold activity, time-delayed feedback, and noise on neuronal firing patterns*, Phys. Rev. E **78**, 041907 (2008).
24. J. Q. Sun and G. Ding: *Advances in Analysis and Control of Time-Delayed Dynamical Systems* (World Scientific, Singapore, 2013).
25. L. M. Pecora and T. L. Carroll: *Master Stability Functions for Synchronized Coupled Systems*, Phys. Rev. Lett. **80**, 2109 (1998).
26. M. Dhamala, V. K. Jirsa, and M. Ding: *Enhancement of neural synchrony by time delay*, Phys. Rev. Lett. **92**, 074104 (2004).
27. C. U. Choe, T. Dahms, P. Hövel, and E. Schöll: *Controlling synchrony by delay coupling in networks: from in-phase to splay and cluster states*, Phys. Rev. E **81**, 025205(R) (2010).
28. W. Kinzel, A. Englert, G. Reents, M. Zigzag, and I. Kanter: *Synchronization of networks of chaotic units with time-delayed couplings*, Phys. Rev. E **79**, 056207 (2009).

29. V. Flunkert, S. Yanchuk, T. Dahms, and E. Schöll: *Synchronizing distant nodes: a universal classification of networks*, Phys. Rev. Lett. **105**, 254101 (2010).
30. S. Heiligenthal, T. Dahms, S. Yanchuk, T. Jüngling, V. Flunkert, I. Kanter, E. Schöll, and W. Kinzel: *Strong and weak chaos in nonlinear networks with time-delayed couplings*, Phys. Rev. Lett. **107**, 234102 (2011).
31. T. Dahms, J. Lehnert, and E. Schöll: *Cluster and group synchronization in delay-coupled networks*, Phys. Rev. E **86**, 016202 (2012).
32. E. Schöll: *Synchronization in delay-coupled complex networks*, in *Advances in Analysis and Control of Time-Delayed Dynamical Systems* (World Scientific, Singapore, 2013), Ed. by J.-Q. Sun, Q. Ding, chap. 4, pp. 57–83.
33. F. Sorrentino and E. Ott: *Network synchronization of groups*, Phys. Rev. E **76**, 056114 (2007).
34. C. R. S. Williams, T. E. Murphy, R. Roy, F. Sorrentino, T. Dahms, and E. Schöll: *Experimental observations of group synchrony in a system of chaotic optoelectronic oscillators*, Phys. Rev. Lett. **110**, 064104 (2013).
35. A. F. Taylor, M. R. Tinsley, F. Wang, and K. Showalter: *Phase clusters in large populations of chemical oscillators*, Angew. Chem. Int. Ed. **50**, 10161 (2011).
36. S. Nkomo, M. R. Tinsley, and K. Showalter: *Chimera states in populations of nonlocally coupled chemical oscillators*, Phys. Rev. Lett. **110**, 244102 (2013).
37. J. Lehnert, P. Hövel, A. A. Selivanov, A. L. Fradkov, and E. Schöll: *Controlling cluster synchronization by adapting the topology*, Phys. Rev. E **90**, 042914 (2014).
38. F. Sorrentino and L. Pecora: *Approximate cluster synchronization in networks with symmetries and parameter mismatches*, Chaos **26**, 094823 (2016).
39. C. Cakan, J. Lehnert, and E. Schöll: *Heterogeneous delays in neural networks*, Eur. Phys. J. B **87**, 54 (2014).
40. Y. N. Kyrychko, K. B. Blyuss, and E. Schöll: *Synchronization of networks of oscillators with distributed-delay coupling*, Chaos **24**, 043117 (2014).
41. C. Wille, J. Lehnert, and E. Schöll: *Synchronization-desynchronization transitions in complex networks: An interplay of distributed time delay and inhibitory nodes*, Phys. Rev. E **90**, 032908 (2014).
42. A. Gjurchinovski, A. Zakharova, and E. Schöll: *Amplitude death in oscillator networks with variable-delay coupling*, Phys. Rev. E **89**, 032915 (2014).
43. A. A. Selivanov, J. Lehnert, T. Dahms, P. Hövel, A. L. Fradkov, and E. Schöll: *Adaptive synchronization in delay-coupled networks of Stuart-Landau oscillators*, Phys. Rev. E **85**, 016201 (2012).
44. S. A. Plotnikov, J. Lehnert, A. L. Fradkov, and E. Schöll: *Adaptive control of synchronization in delay-coupled heterogeneous networks of FitzHugh-Nagumo nodes*, Int. J. Bifurc. Chaos **26**, 1650058 (2016).
45. J. Lehnert, T. Dahms, P. Hövel, and E. Schöll: *Loss of synchronization in complex neural networks with delay*, Europhys. Lett. **96**, 60013 (2011).
46. A. Keane, T. Dahms, J. Lehnert, S. A. Suryanarayana, P. Hövel, and E. Schöll: *Synchronisation in networks of delay-coupled type-I excitable systems*, Eur. Phys. J. B **85**, 407 (2012).
47. G. Saxena, A. Prasad, and R. Ramaswamy: *Amplitude death: The emergence of stationarity in coupled nonlinear systems*, Phys. Rep. **521**, 205 (2012).
48. A. Koseska, E. Volkov, and J. Kurths: *Oscillation quenching mechanisms: Amplitude vs. oscillation death*, Phys. Rep. **531**, 173 (2013).
49. A. Zakharova, I. Schneider, Y. N. Kyrychko, K. B. Blyuss, A. Koseska, B. Fiedler, and E. Schöll: *Time delay control of symmetry-breaking primary and secondary oscillation death*, Europhys. Lett. **104**, 50004 (2013).
50. I. Schneider, M. Kapeller, S. Loos, A. Zakharova, B. Fiedler, and E. Schöll: *Stable and transient multi-cluster oscillation death in nonlocally coupled networks*, Phys. Rev. E **92**, 052915 (2015).
51. F. M. Atay: *Total and partial amplitude death in networks of diffusively coupled oscillators*, Physica D **183**, 1 (2002).
52. L. L. Rubchinsky, M. M. Sushchik, and G. V. Osipov: *Patterns in networks of oscillators formed via synchronization and oscillator death*, Math. Comp. Simul **58**, 443 (2002).
53. A. L. Do, J. M. Höfener, and T. Gross: *Engineering mesoscale structures with distinct dynamical implications*, New J. Phys. **14**, 115022 (2012).
54. L. M. Pecora, F. Sorrentino, A. M. Hagerstrom, T. E. Murphy, and R. Roy: *Symmetries, cluster synchronization, and isolated desynchronization in complex networks*, Nat. Commun. **5**, 4079 (2014).

55. W. Poel, A. Zakharova, and E. Schöll: *Partial synchronization and partial amplitude death in mesoscale network motifs*, Phys. Rev. E **91**, 022915 (2015).
56. F. Sorrentino, L. M. Pecora, A. M. Hagerstrom, T. E. Murphy, and R. Roy: *Complete characterization of the stability of cluster synchronization in complex dynamical networks*, Sci. Adv. **2**, e1501737 (2016).
57. S. Krishnagopal, J. Lehnert, W. Poel, A. Zakharova, and E. Schöll: *Synchronization patterns: From network motifs to hierarchical networks*, Phil. Trans. R. Soc. A **375**, 20160216 (2017).
58. M. J. Panaggio and D. M. Abrams: *Chimera states: Coexistence of coherence and incoherence in networks of coupled oscillators*, Nonlinearity **28**, R67 (2015).
59. E. Schöll: *Synchronization patterns and chimera states in complex networks: interplay of topology and dynamics*, Eur. Phys. J. Spec. Top. **225**, 891 (2016).
60. Y. Kuramoto and D. Battogtokh: *Coexistence of Coherence and Incoherence in Nonlocally Coupled Phase Oscillators.*, Nonlin. Phen. in Complex Sys. **5**, 380 (2002).
61. D. M. Abrams and S. H. Strogatz: *Chimera states for coupled oscillators*, Phys. Rev. Lett. **93**, 174102 (2004).
62. N. C. Rattenborg, C. J. Amlaner, and S. L. Lima: *Behavioral, neurophysiological and evolutionary perspectives on unihemispheric sleep*, Neurosci. Biobehav. Rev. **24**, 817 (2000).
63. N. C. Rattenborg, B. Voirin, S. M. Cruz, R. Tisdale, G. Dell'Omo, H. P. Lipp, M. Wikelski, and A. L. Vyssotski: *Evidence that birds sleep in mid-flight*, Nat. Commun. **7**, 12468 (2016).
64. L. Ramlow, J. Sawicki, A. Zakharova, J. Hlinka, J. C. Claussen, and E. Schöll: *Partial synchronization in empirical brain networks as a model for unihemispheric sleep* (2019), arXiv:1904.05949.
65. P. Jiruska, M. de Curtis, J. G. R. Jefferys, C. A. Schevon, S. J. Schiff, and K. Schindler: *Synchronization and desynchronization in epilepsy: controversies and hypotheses*, J. Physiol. **591.4**, 787 (2013).
66. V. K. Jirsa, W. C. Stacey, P. P. Quilichini, A. I. Ivanov, and C. Bernard: *On the nature of seizure dynamics*, Brain **137**, 2210 (2014).
67. A. Rothkegel and K. Lehnertz: *Irregular macroscopic dynamics due to chimera states in small-world networks of pulse-coupled oscillators*, New J. Phys. **16**, 055006 (2014).
68. R. G. Andrzejak, C. Rummel, F. Mormann, and K. Schindler: *All together now: Analogies between chimera state collapses and epileptic seizures*, Sci. Rep. **6**, 23000 (2016).
69. T. Chouzouris, I. Omelchenko, A. Zakharova, J. Hlinka, P. Jiruska, and E. Schöll: *Chimera states in brain networks: empirical neural vs. modular fractal connectivity*, Chaos **28**, 045112 (2018).
70. J. C. Gonzalez-Avella, M. G. Cosenza, and M. S. Miguel: *Localized coherence in two interacting populations of social agents*, Physica A **399**, 24 (2014).
71. A. Gjurchinovski, E. Schöll, and A. Zakharova: *Control of amplitude chimeras by time delay in dynamical networks*, Phys. Rev. E **95**, 042218 (2017).
72. J. Sawicki, I. Omelchenko, A. Zakharova, and E. Schöll: *Chimera states in complex networks: interplay of fractal topology and delay*, Eur. Phys. J. Spec. Top. **226**, 1883 (2017).
73. A. Zakharova, N. Semenova, V. S. Anishchenko, and E. Schöll: *Time-delayed feedback control of coherence resonance chimeras*, Chaos **27**, 114320 (2017).
74. J. Sawicki, I. Omelchenko, A. Zakharova, and E. Schöll: *Delay-induced chimeras in neural networks with fractal topology*, Eur. Phys. J. B **92**, 54 (2019).
75. S. Boccaletti, G. Bianconi, R. Criado, C. I. del Genio, J. Gómez-Gardeñes, M. Romance, I. Sendiña Nadal, Z. Wang, and M. Zanin: *The structure and dynamics of multilayer networks*, Phys. Rep. **544**, 1 (2014).
76. M. De Domenico, A. Solé-Ribalta, E. Cozzo, M. Kivelä, Y. Moreno, M. A. Porter, S. Gómez, and A. Arenas: *Mathematical formulation of multilayer networks*, Phys. Rev. X **3**, 041022 (2013).
77. M. De Domenico, V. Nicosia, A. Arenas, and V. Latora: *Structural reducibility of multilayer networks*, Nat. Commun. **6**, 6864 (2015).
78. M. Kivelä, A. Arenas, M. Barthélemy, J. P. Gleeson, Y. Moreno, and M. A. Porter: *Multilayer networks*, J. Complex Networks **2**, 203 (2014).
79. B. Bentley, R. Branicky, C. L. Barnes, Y. L. Chew, E. Yemini, E. T. Bullmore, P. E. Vétes, and W. R. Schafer: *The multilayer connectome of caenorhabditis elegans*, PLOS Comput. Biol. **12**, 1 (2016).
80. F. Battiston, V. Nicosia, M. Chavez, and V. Latora: *Multilayer motif analysis of brain networks*, Chaos **27**, 047404 (2017).
81. X. Zhang, S. Boccaletti, S. Guan, and Z. Liu: *Explosive synchronization in adaptive and multilayer networks*, Phys. Rev. Lett. **114**, 038701 (2015).

82. V. A. Maksimenko, V. V. Makarov, B. K. Bera, D. Ghosh, S. K. Dana, M. V. Goremyko, N. S. Frolov, A. A. Koronovskii, and A. E. Hramov: *Excitation and suppression of chimera states by multiplexing*, Phys. Rev. E **94**, 052205 (2016).
83. S. Jalan and A. Singh: *Cluster synchronization in multiplex networks*, Europhys. Lett. **113**, 30002 (2016).
84. S. Ghosh and S. Jalan: *Emergence of chimera in multiplex network*, Int. J. Bifurc. Chaos **26**, 1650120 (2016).
85. I. Leyva, R. Sevilla-Escoboza, I. Sendiña-Nadal, R. Gutiérrez, J. M. Buldú, and S. Boccaletti: *Inter-layer synchronization in non-identical multi-layer networks*, Sci. Rep. **7**, 45475 (2017).
86. R. G. Andrzejak, G. Ruzzene, and I. Malvestio: *Generalized synchronization between chimera states*, Chaos **17**, 053114 (2017).
87. R. FitzHugh: *Impulses and physiological states in theoretical models of nerve membrane*, Biophys. J. **1**, 445 (1961).
88. J. Nagumo, S. Arimoto, and S. Yoshizawa.: *An active pulse transmission line simulating nerve axon.*, Proc. IRE **50**, 2061 (1962).
89. E. M. Izhikevich: *Which model to use for cortical spiking neurons?*, IEEE Transactions on Neural Networks **15**, 1063 (2004).
90. E. Schöll, G. Hiller, P. Hövel, and M. A. Dahlem: *Time-delayed feedback in neurosystems*, Phil. Trans. R. Soc. A **367**, 1079 (2009).
91. S. A. Brandstetter, M. A. Dahlem, and E. Schöll: *Interplay of time-delayed feedback control and temporally correlated noise in excitable systems*, Philos. Trans. Royal Soc. A **368**, 391 (2010).
92. I. Omelchenko, O. E. Omel'chenko, P. Hövel, and E. Schöll: *When nonlocal coupling between oscillators becomes stronger: patched synchrony or multichimera states*, Phys. Rev. Lett. **110**, 224101 (2013).
93. P. Katsaloulis, A. Ghosh, A. C. Philippe, A. Provata, and R. Deriche: *Fractality in the neuron axonal topography of the human brain based on 3-D diffusion MRI*, Eur. Phys. J. B **85**, 1 (2012).
94. D. Ning, X. Wu, J. Lu, and J. Lü: *Driving-based generalized synchronization in two-layer networks via pinning control*, Chaos **25**, 113104 (2015).
95. A. L. Fradkov: *Speed-gradient scheme and its application in adaptive control problems*, Autom. Remote Control **40**, 1333 (1979).
96. A. L. Fradkov: *Cybernetical Physics: From Control of Chaos to Quantum Control* (Springer, Heidelberg, Germany, 2007).
97. I. Omelchenko, A. Provata, J. Hizanidis, E. Schöll, and P. Hövel: *Robustness of chimera states for coupled FitzHugh-Nagumo oscillators*, Phys. Rev. E **91**, 022917 (2015).
98. S. Ulonska, I. Omelchenko, A. Zakharova, and E. Schöll: *Chimera states in networks of Van der Pol oscillators with hierarchical connectivities*, Chaos **26**, 094825 (2016).
99. A. E. Pereda: *Electrical synapses and their functional interactions with chemical synapses*, Nature **15**, 250 (2014).
100. D. P. Rosin, K. E. Callan, D. J. Gauthier, and E. Schöll: *Pulse-train solutions and excitability in an optoelectronic oscillator*, Europhys. Lett. **96**, 34001 (2011).
101. T. Erneux, L. Weicker, L. Bauer, and P. Hövel: *Short-time-delay limit of the self-coupled FitzHugh-Nagumo system*, Phys. Rev. E **93**, 022208 (2016).
102. A. Panchuk, D. P. Rosin, P. Hövel, and E. Schöll: *Synchronization of coupled neural oscillators with heterogeneous delays*, Int. J. Bifurcation Chaos **23**, 1330039 (2013).